

A RE-EVALUATION OF THE STRUCTURE OF WEEKSITE, A URANYL SILICATE FRAMEWORK MINERAL

JENNIFER M. JACKSON[§] AND PETER C. BURNS

*Department of Civil Engineering and Geological Sciences, 156 Fitzpatrick Hall,
University of Notre Dame, Notre Dame, Indiana 46556, U.S.A.*

ABSTRACT

The structure of weeksite, $K_{1.26}Ba_{0.25}Ca_{0.12}[(UO_2)_2(Si_5O_{13})]H_2O$, orthorhombic, a 14.209(2), b 14.248(2), c 35.869(4) Å, V 7262(2) Å³, space group *Cmmb*, has been solved by direct methods using data collected with MoK α X-radiation and a CCD-based detector and refined by full-matrix least-squares techniques, on the basis of F^2 for all unique reflections, to an agreement factor (R_1) of 7.0% and a goodness-of-fit (S) of 1.04, calculated using the 1565 unique observed reflections ($F_o \leq 4\sigma_F$). The structure contains four unique U^{6+} positions, each of which is part of a nearly linear $(UO_2)^{2+}$ uranyl ion. The uranyl ions (Ur) are further coordinated by five atoms of oxygen arranged at the equatorial corners of UrO_5 pentagonal bipyramids. There are ten silicon atoms, each of which is tetrahedrally coordinated by oxygen atoms. The uranyl polyhedra share equatorial edges to form chains, which in turn share polyhedron edges with silicate tetrahedra. The uranyl silicate chains are linked to crankshaft-like chains of vertex-sharing silicate tetrahedra, resulting in layers that are connected by the sharing of vertices between silicate tetrahedra to form an open framework. Potassium, barium, calcium and H_2O are located in the channels within the uranyl silicate framework. Displacement of some atoms from their corresponding special positions indicates that the results represent an average structure.

Keywords: weeksite, uranyl silicate, structure determination, open framework.

SOMMAIRE

Nous avons résolu la structure de la weeksite, $K_{1.26}Ba_{0.25}Ca_{0.12}[(UO_2)_2(Si_5O_{13})]H_2O$, orthorhombique, a 14.209(2), b 14.248(2), c 35.869(4) Å, V 7262(2) Å³, groupe spatial *Cmmb*, par méthodes directes; les données ont été prélevées avec rayonnement MoK α et un détecteur de type CCD, et affinées sur matrice entière par moindres carrés, sous forme de facteurs F^2 pour toutes réflexions uniques, jusqu'à un résidu (R_1) de 7.0% et un indice de concordance (S) de 1.04, calculés sur une base de 1565 réflexions uniques observées ($F_o \leq 4\sigma_F$). La structure contient quatre positions U^{6+} uniques, chacune faisant partie d'un ion uranyle $(UO_2)^{2+}$ presque linéaire. Les ions uranyle (Ur) sont de plus liés à cinq atomes d'oxygène disposés aux coins équatoriaux de bipyramides pentagonales UrO_5 . Il y a dix atomes de silicium, chacun entouré de quatre atomes d'oxygène. Le polyèdre à uranyle partage ses arêtes équatoriales pour former des chaînes, qui à leur tour partagent des arêtes avec des tétraèdres de silice. Les chaînes contenant les tétraèdres et l'uranyle sont liées à des chaînes ressemblant à un vilebrequin faites de tétraèdres de silice à coins partagés, le tout formant des feuillets connectés par partage de coins entre tétraèdres pour former une trame ouverte. Le potassium, barium, calcium et les groupes H_2O occupent des canaux dans la trame. D'après le déplacement de certains atomes par rapport à leurs positions spéciales correspondantes, nos résultats se rapportent à une structure moyenne.

(Traduit par la Rédaction)

Mots-clés: weeksite, silicate d'uranyle, détermination de la structure, trame ouverte.

[§] *Present address:* Department of Geology, 245 Natural History Building, University of Illinois, 1301 W. Green Street, Urbana, Illinois 61801, U.S.A. *E-mail address:* jmjackso@uiuc.edu.

INTRODUCTION

Uranyl silicates are common constituents of the oxidized portions of uranium deposits in Si-rich rocks (Fron del 1958, Finch & Ewing 1992, Percy *et al.* 1994, Finch & Murakami 1999) and are important for understanding the genesis of such deposits. Fourteen uranyl silicates have been described as minerals (Mandarino 1999). Uranyl silicates are dominated by the uranophane group, which includes nine species with a U:Si ratio of 1:1. Haiweeite, $\text{Ca}[(\text{UO}_2)_2\text{Si}_5\text{O}_{12}(\text{OH})_2](\text{H}_2\text{O})_3$, and weeksite have U:Si ratios of 2:5, and their structures are substantially different from that of other uranyl silicates (Burns *et al.* 1996, Burns 2001).

Uranyl silicates are likely to be abundant in a geological repository for nuclear waste, owing to the alteration of spent nuclear fuel and borosilicate waste glass in the presence of silicon derived from repository host-rocks. Uranophane, $\text{Ca}[(\text{UO}_2)_2(\text{SiO}_3\text{OH})_2](\text{H}_2\text{O})_5$, and boltwoodite, $(\text{K},\text{Na})[(\text{UO}_2)(\text{SiO}_3\text{OH})](\text{H}_2\text{O})_{1.5}$, are dominant phases associated with the alteration of spent nuclear fuel in high-drip-rate tests using modified groundwater (EJ-13) from the Yucca Mountain site (Finch *et al.* 1999). Both phases also were found in similar tests using unirradiated UO_2 (Wronkiewicz *et al.* 1996). Haiweeite was tentatively identified in corrosion tests involving spent fuel by Wilson (1990). Weeksite was identified as an alteration phase in batch tests by Buck & Fortner (1997) using modified groundwater (EJ-13) and actinide-bearing borosilicate waste glass. Recently, Burns *et al.* (2000) reported that weeksite forms on actinide-bearing borosilicate waste glass subjected to hydrous vapor-induced alteration. We consider it likely that uranyl compounds that may form by the alteration of nuclear waste will incorporate radionuclides into their crystal structures, thereby retarding their release (Burns *et al.* 1997b, Burns 1999, Chen *et al.* 1999, 2000, Burns *et al.* 2000). Thus, an understanding of the structures of uranyl silicates may be a key to understanding the long-term performance of a geological repository for nuclear waste. Here we report the results of a redetermination of the structure of weeksite.

PREVIOUS STUDIES OF WEEKSITE

Crystallographic data for weeksite were provided by Drs. Joan Clark and George Ashby of the U.S. Geological Survey, and were reported by Outerbridge *et al.* (1960): space group *Pnmb*, a 14.26(2), b 35.88(10), c 14.20(2) Å. Outerbridge *et al.* (1960) indicated that the structure has strong pseudosymmetry. Stohl & Smith (1981) reported a partial structure for weeksite, with the coordinates given on the subcell a 7.106(8), b 17.90(2), c 7.087(7) Å, space group *Amm2*, with a final agreement index (R) of 15%. Baturin & Sidorenko (1985) provided a model based upon a similar subcell and with the location of all Si atoms, but space group *Cmmm*,

with a final R of 12%. In both cases, the authors noted the presence of a larger unit-cell.

EXPERIMENTAL

X-ray diffraction

The crystals of weeksite studied are from the Anderson mine, Yavapai County, Arizona. The specimen contains radiating aggregates of acicular crystals of weeksite, with individual crystals up to ~0.2 mm long and ~0.05 mm wide. A crystal that exhibits uniform optical properties and sharp extinction between crossed polarizers, with approximate dimensions $0.03 \times 0.05 \times 0.19$ mm, was selected and mounted on a Bruker PLATFORM 3-circle goniometer equipped with a 1K SMART CCD (charge-coupled device) detector and a crystal-to-detector distance of 5 cm. Burns (1998) provided a discussion of the application of CCD detectors to the analysis of mineral structures.

A sphere of data was collected using monochromatic $\text{MoK}\alpha$ X-radiation and frame widths of 0.3° in ω , with 30 s used to acquire each frame. Several hundred frames of data were analyzed to locate diffraction maxima for determination of the unit cell. All peaks were found to be consistent with an orthorhombic *C*-centered unit cell using an $1/3\sigma$ cut-off, with dimensions a 14.209(2), b 14.248(2), c 35.869(4) Å (Table 1); these were refined using least-squares techniques and 6022 reflections. Diffraction peaks were found to be sharp, and the pattern does not display evidence of twinning. Data were collected for $3^\circ \leq 2\theta \leq 56.64^\circ$ in approximately 24 hours; comparison of the intensities of identical reflections collected at different times during the data collection showed no evidence of decay. The three-dimensional data were integrated and corrected for Lorentz, polarization, and background effects using the Bruker program SAINT. A semi-empirical absorption correction was done on the basis of the intensities of equivalent reflections, with the crystal modeled as an ellipsoid. A total of 2245 reflections was employed for parameter estimation, and the correction lowered R_{INT} of the 2245 reflections from 17.6% to 7.7%. A total of 65,488 intensities was measured, with 32,666 consis-

TABLE 1. MISCELLANEOUS INFORMATION CONCERNING WEEKSITE

| | | | |
|---|-------------|-------------------------------|--------------------------------|
| a (Å) | 14.209(2) | Crystal size (mm) | $0.03 \times 0.05 \times 0.19$ |
| b (Å) | 14.248(2) | Total ref. | 32,666 |
| c (Å) | 35.869(4) | Unique ref. | 4845 |
| V (Å ³) | 7262(2) | R_{INT} (%) | 10.2 |
| Space group | <i>Cmmm</i> | Unique $ F_o \geq 4\sigma_F$ | 1565 |
| $F(000)$ | 7045.44 | Final R_1 (%) | 7.0 |
| μ (mm ⁻¹) | 19.09 | S | 1.04 |
| D_{calc} (g/cm ³) | 3.640 | | |
| Unit cell contents: $16\{\text{K}_{1.2}\text{Ba}_{0.2}\text{Ca}_{0.12}[(\text{UO}_2)_2(\text{Si}_5\text{O}_{12})(\text{Si}_2\text{O}_7)]\text{H}_2\text{O}\}$ | | | |
| $R_1 = \sum(F_o - F_c) / \sum F_o \times 100$ | | | |
| $S = [\sum w(F_o - F_c)^2 / (m - n)]^{1/2}$, for m observations and n parameters | | | |

tent with the *C*-centered lattice. Merging of equivalent reflections gave 4845 unique reflections (R_{INT} of all data = 10.2%) with 1565 classed as observed ($F_O \geq 4\sigma_F$).

Electron-microprobe analysis (EMPA)

Two single crystals of weeksite, from the same bulk sample as the crystal used for the collection of the X-ray-diffraction data, were mounted in epoxy, polished, and coated with carbon. Electron-microprobe analyses (EMPA) were performed using a Cameca SX-50 instrument in wavelength-dispersion spectroscopy (WDS) mode. Data were reduced using the method of Pouchou & Pichoir (1984).

All analyses were performed with an accelerating voltage of 15 kV and a probe current of 25 nA. In order to minimize alkali migration, a defocused beam 10 μm in diameter was used. Counting times on peak and background were 40 s for BaK α , 30 s for NaK α , CaK α , and SrK α , and 10 s for SiK α , KK α and UM α . The proportion of oxygen was calculated on the basis of stoichiometry using assumed valences for the cations. At these conditions, no significant migration of Na, K or Ca could be detected. A 100-s energy-dispersion scan indicated no elements with *Z* greater than eight, other than those reported herein. The following analytical EMPA standards were used: paracelsian (BaK α), Amelia albite (NaK α), anorthite glass (CaK α , SiK α), Sr-substituted anorthite (SrK α), microcline (KK α), and synthetic UO₂ from Oak Ridge National Laboratory (UM α). Identical analytical conditions were used to analyze both standards and the crystals of weeksite. The proportion of H₂O was assumed to provide an analytical total of 100%.

STRUCTURE SOLUTION AND REFINEMENT

Scattering curves for neutral atoms, together with anomalous dispersion corrections, were taken from *International Tables for X-Ray Crystallography, Vol. IV* (Ibers & Hamilton 1974). The Bruker SHELXTL Version 5 system of programs was used for the determination and refinement of the structure.

Systematic absences and reflection statistics are consistent with space group *Cmmb*, with no violations of the *b* glide. The structure was solved and refined in *Cmmb*. However, some cations were found to be displaced from their corresponding special positions, indicating an average structure, so we also considered space groups *Cmmm*, *C2mm* and *C222*. Satisfactory solutions of the structure could not be obtained in any of these space groups. The possibility of the existence of a larger unit-cell was investigated by carefully examining the CCD-detector-collected data, but no reflections were found to support this possibility. The structural model was refined on the basis of F^2 using all unique data. The displacement parameters for all U and M (*M*: low-

valence cation) sites were converted to anisotropic forms, and were refined, together with the positional parameters for all atoms and a weighting scheme of the structure factors, resulting in a final R_1 index of 7.0%, calculated for the 1565 unique observed reflections ($F_O \geq 4\sigma_F$), and a goodness-of-fit (*S*) of 1.04. In the final cycle of refinement, the average parameter shift/esd was 0.000. The final atomic-positional parameters and anisotropic-displacement parameters are given in Tables 2 and 3, respectively. Selected interatomic distances and angles are given in Table 4. A bond-valence table, as well as observed and calculated structure-factors, are available from the Depository of Unpublished Data, CISTI, National Research Council, Ottawa, Ontario K1A 0S2, Canada.

TABLE 2. FINAL ATOMIC PARAMETERS FOR WEEKSITE

| | <i>x</i> | <i>y</i> | <i>z</i> | * U_{eq} |
|----------------------|------------|-----------|------------|------------|
| U(1) | ¼ | 0.2543(1) | 0.15016(3) | 133(3) |
| U(2) | ¼ | 0.2545(1) | 0.34843(3) | 189(4) |
| U(3) | 0 | ¼ | 0.40027(4) | 219(4) |
| U(4) | 0 | ¼ | 0.09875(3) | 139(3) |
| Si(1) | ¼ | 0.1937(4) | 0.2496(2) | 50(11) |
| Si(2) | 0.0487(3) | 0.1100(3) | 0.2491(2) | 72(8) |
| Si(3) | ¼ | 0.2517(8) | 0.4371(3) | 233(22) |
| Si(4) | ¼ | 0.2494(7) | 0.0627(2) | 112(17) |
| Si(5) | 0 | ¼ | 0.1863(3) | 164(19) |
| Si(6) | 0 | ¼ | 0.3117(3) | 186(21) |
| Si(7)** | 0 | 0.190(1) | 0 | 196(36) |
| Si(8)** | -0.2031(9) | 0.1102(9) | 0.0001(4) | 209(25) |
| Si(9)** | 0 | 0.193(2) | ½ | 350(50) |
| Si(10)** | 0.201(1) | 0.110(1) | 0.5000(5) | 343(33) |
| M(1) | 0.0888(6) | ½ | 0.1602(3) | 373(28) |
| M(2) | 0.9114(7) | 0 | 0.3376(3) | 445(32) |
| M(3) | 0.160(1) | 0 | 0.4161(7) | 638(76) |
| M(4) | 0.841(1) | 0 | 0.4092(5) | 406(55) |
| M(5) | 0.159(1) | ½ | 0.0890(5) | 402(48) |
| M(6) | 0.157(1) | 0 | 0.0836(6) | 634(74) |
| O(1) | ¼ | 0.261(2) | 0.2132(6) | 279(57) |
| O(2) | 0 | ¼ | -0.0369(6) | 260(55) |
| O(3) | ¼ | 0.258(2) | 0.2858(6) | 258(54) |
| O(4) | 0 | ¼ | 0.4626(8) | 434(76) |
| O(5) | -0.162(1) | 0.248(1) | 0.0898(5) | 244(37) |
| O(6) | 0.1605(8) | 0.1228(7) | 0.2489(4) | 159(24) |
| O(7) | -0.089(1) | 0.754(1) | 0.1576(5) | 250(38) |
| O(8) | 0.088(1) | 0.260(1) | 0.3408(4) | 222(37) |
| O(9) | 0.002(1) | 0.159(1) | 0.2134(5) | 251(39) |
| O(10) | 0.004(2) | 0.154(1) | 0.2866(5) | 386(49) |
| O(11) | ¼ | 0.160(2) | 0.4632(8) | 350(74) |
| O(12) | 0.161(1) | 0.250(1) | 0.4089(5) | 294(41) |
| O(13) | ¼ | 0.381(2) | 0.1463(6) | 146(48) |
| O(14) | ¼ | 0.383(2) | 0.3503(7) | 367(78) |
| O(15) | 0.000(2) | 0.126(1) | 0.0993(5) | 314(45) |
| O(16) | ¼ | 0.129(2) | 0.1499(6) | 202(59) |
| O(17) | ¼ | 0.126(2) | 0.3465(8) | 505(96) |
| O(18) | -0.001(2) | 0.124(2) | 0.3994(5) | 371(48) |
| O(19) | 0.025(1) | 0 | 0.2491(5) | 101(30) |
| O(20) | ¼ | 0.157(2) | 0.0364(7) | 250(61) |
| O(21) | -¼ | 0.158(2) | 0.0361(6) | 192(55) |
| O(22) | ¼ | 0.341(2) | 0.4633(9) | 467(89) |
| O(23) | ¼ | 0 | 0.498(2) | 675(147) |
| O(24) | -¼ | 0 | 0.002(2) | 687(150) |
| O(25)** | -0.091(2) | 0.119(2) | 0.000(1) | 301(77) |
| O(26)** | 0.090(3) | 0.126(3) | 0.500(1) | 550(117) |
| H ₂ O(27) | -0.106(3) | ½ | 0.168(1) | 140(99) |
| H ₂ O(28) | ¼ | ½ | 0.249(2) | 3121(312) |

* $U_{eq} = U_{eq} \text{ \AA}^2 \times 10^4$, **positions 50% occupied

RESULTS

Projection of the structure of weeksite along [100] reveals layers of uranyl polyhedra and silicate tetrahedra parallel to (010), with cations [$M(1)$ to $M(6)$] and H_2O groups located in channels of an open framework formed by cross-linking of the uranyl silicate layer (Fig. 1). The structure reported herein confirms the generalities of the substructure reported by Baturin & Sidorenko (1985), but was determined for a larger cell and a different space-group, and has resulted in a lower R and a more precisely characterized structure.

Cation polyhedra

The structure of weeksite contains four symmetrically distinct U^{6+} cations, each of which is strongly bonded to two atoms of O, forming nearly linear $(UO_2)^{2+}$ uranyl ions (Ur) with $U-O_{Ur}$ bond-lengths ≈ 1.8 Å, as is normally the case in structures that contain U^{6+} (Burns *et al.* 1997a). Each U^{6+} cation is coordinated by five additional atoms of O that are arranged at the equatorial corners of pentagonal bipyramids (O_{eq}) capped by the O_{Ur} atoms. The uranyl pentagonal bipyramid is the only coordination polyhedron observed about U^{6+} in uranyl silicate minerals (Burns *et al.* 1996), although synthetic uranyl silicates also contain uranyl square bipyramids (Burns *et al.* 2000). The $\langle U-O_{eq} \rangle$ bond-lengths are 2.37, 2.38, 2.36 and 2.36 Å for the U(1), U(2), U(3) and U(4) sites, respectively; they compare favorably with the average of 2.37(9) Å obtained from a large number of well-refined structures that contain uranyl pentagonal bipyramids (Burns *et al.* 1997a). The bond-valence sums incident at the U positions, calculated using the parameters proposed by Burns *et al.* (1997a), range from 5.75 to 6.12 *vu*.

There are ten symmetrically distinct Si positions, each of which is tetrahedrally coordinated by four atoms of O (Table 4). The Si(7), Si(8), Si(9) and Si(10) sites are displaced from their corresponding special positions. The Si(7) site is displaced from the $4a$ position, with a Si(7)–Si(7) separation of 1.72(4) Å. The Si(9)

TABLE 3. ANISOTROPIC DISPLACEMENT PARAMETERS FOR WEEKSITE

| | U_{11} | U_{22} | U_{33} | U_{12} | U_{13} | U_{23} |
|--------|----------|----------|----------|----------|-----------|----------|
| U(1) | 94(6) | 181(6) | 124(6) | 0 | 0 | -18(4) |
| U(2) | 141(7) | 317(8) | 108(7) | 0 | 0 | -41(5) |
| U(3) | 152(7) | 405(9) | 99(6) | 9(9) | 0 | 0 |
| U(4) | 98(6) | 179(6) | 141(7) | -6(7) | 0 | 0 |
| $M(1)$ | 184(50) | 392(49) | 544(59) | 0 | 7(39) | 0 |
| $M(2)$ | 274(58) | 437(53) | 623(66) | 0 | 65(46) | 0 |
| $M(3)$ | 529(134) | 531(124) | 854(159) | 0 | -397(115) | 0 |
| $M(4)$ | 462(121) | 328(94) | 429(98) | 0 | 20(83) | 0 |
| $M(5)$ | 195(77) | 293(80) | 718(118) | 0 | -20(74) | 0 |
| $M(6)$ | 705(155) | 329(96) | 869(158) | 0 | 210(118) | 0 |

$$*U_{ij} = U_{ij} \text{ \AA}^2 \times 10^4$$

TABLE 4. SELECTED INTERATOMIC DISTANCES (Å) AND ANGLES (°) FOR WEEKSITE

| | | | | |
|-------------------------------|----------|---------------|----------------------|----------|
| U(1)-O(16) | 1.79(2) | Si(1)-O(3) | 1.59(2) | |
| U(1)-O(13) | 1.82(2) | Si(1)-O(6),f | 1.62(1) | x2 |
| U(1)-O(1) | 2.26(2) | Si(1)-O(1) | 1.61(2) | |
| U(1)-O(7)c,g | 2.30(2) | <Si(1)-O> | 1.61 | |
| U(1)-O(5)b,m | 2.50(2) | | | |
| <U(1)-O _{ur} > | 1.81 | Si(2)-O(10) | 1.61(2) | |
| <U(1)-O _{eq} > | 2.37 | Si(2)-O(19) | 1.60(1) | |
| O(13)-U(1)-O(16) | 175.3(9) | Si(2)-O(6) | 1.60(1) | |
| | | Si(2)-O(9) | 1.61(2) | |
| | | <Si(2)-O> | 1.61 | |
| U(2)-O(14) | 1.84(3) | | | |
| U(2)-O(17) | 1.83(3) | | | |
| U(2)-O(3) | 2.25(2) | Si(3)-O(22) | 1.59(3) | |
| U(2)-O(8),f | 2.32(2) | Si(3)-O(11) | 1.62(3) | |
| U(2)-O(12),f | 2.51(2) | Si(3)-O(12),f | 1.62(2) | x2 |
| <U(2)-O _{ur} > | 1.84 | <Si(3)-O> | 1.61 | |
| <U(2)-O _{eq} > | 2.38 | | | |
| O(17)-U(2)-O(14) | 180(1) | Si(4)-O(5)m,b | 1.59(2) | x2 |
| | | Si(4)-O(21)b | 1.64(2) | |
| | | Si(4)-O(20) | 1.62(2) | |
| | | <Si(4)-O> | 1.61 | |
| U(3)-O(18) | 1.79(2) | x2 | | |
| U(3)-O(4) | 2.24(3) | | | |
| U(3)-O(12),b | 2.30(2) | x2 | | |
| U(3)-O(8),b | 2.48(2) | x2 | Si(5)-O(9),b | 1.61(2) |
| <U(3)-O _{ur} > | 1.79 | | Si(5)-O(7)n,g | 1.63(2) |
| <U(3)-O _{eq} > | 2.36 | | <Si(5)-O> | 1.62 |
| O(18)b-U(3)-O(18) | 178(1) | | | |
| | | Si(6)-O(8),b | 1.63(2) | x2 |
| | | Si(6)-O(10),b | 1.64(2) | x2 |
| | | <Si(6)-O> | 1.64 | |
| U(4)-O(15),b | 1.77(2) | x2 | | |
| U(4)-O(2)h | 2.22(2) | | | |
| U(4)-O(5),b | 2.32(2) | x2 | | |
| U(4)-O(7)g,n | 2.46(2) | x2 | Si(7)-O(2),h | 1.58(2) |
| <U(4)-O _{ur} > | 1.77 | | Si(7)-O(25),j | 1.64(4) |
| <U(4)-O _{eq} > | 2.36 | | <Si(7)-O> | 1.61 |
| O(15)-U(4)-O(15)b | 179(1) | | | |
| | | Si(8)-O(25) | 1.60(4) | |
| $M(1)$ -H ₂ O(27) | 2.78(4) | x2 | Si(8)-O(20)p | 1.61(3) |
| $M(1)$ -O(13),a | 2.89(1) | x2 | Si(8)-O(21) | 1.60(2) |
| $M(1)$ -O(15)b,i | 3.10(2) | x2 | Si(8)-O(24) | 1.71(1) |
| $M(1)$ -O(9)b,i | 3.24(2) | x2 | <Si(8)-O> | 1.63 |
| < $M(1)$ - ϕ > | 3.03 | | | |
| $M(2)$ -O(8)d,r | 3.42(2) | x2 | Si(9)-O(26),q | 1.59(5) |
| $M(2)$ -O(14)c,d | 2.87(2) | x2 | Si(9)-O(4),l | 1.57(3) |
| $M(2)$ -O(18)e,o | 3.10(2) | x2 | <Si(9)-O> | 1.60 |
| $M(2)$ -O(10)e,o | 3.15(2) | x2 | | |
| < $M(2)$ - ϕ > | 3.14 | | Si(10)-O(22)k | 1.64(3) |
| | | | Si(10)-O(11) | 1.65(3) |
| $M(3)$ -O(18) | 2.95(3) | x2 | Si(10)-O(26) | 1.59(5) |
| $M(3)$ -O(11),s | 3.11(3) | x2 | Si(10)-O(23) | 1.72(2) |
| $M(3)$ -O(23) | 3.20(5) | | <Si(10)-O> | 1.65 |
| $M(3)$ -O(17),s | 3.33(4) | x2 | | |
| < $M(3)$ - ϕ > | 3.14 | | O(3)-Si(1)-O(6),f | 111.7(8) |
| | | | O(3)-Si(1)-O(1) | 109(1) |
| $M(4)$ -O(18)e,o | 2.88(3) | x2 | O(6)-Si(1)-O(6),f | 103.1(8) |
| $M(4)$ -O(14)c,d | 2.99(3) | x2 | O(6),f-Si(1)-O(1) | 110.8(8) |
| $M(4)$ -O(22)c,d | 3.25(3) | x2 | <O-Si(1)-O> | 109.5 |
| < $M(4)$ - ϕ > | 3.04 | | | |
| | | | O(10)-Si(2)-O(19) | 107(1) |
| $M(5)$ -O(15)b,i | 2.91(2) | x2 | O(10)-Si(2)-O(6) | 111(1) |
| $M(5)$ -O(13),a | 2.96(2) | x2 | O(10)-Si(2)-O(9) | 109.5(9) |
| $M(5)$ -O(21)b,w | 3.21(2) | x2 | O(19)-Si(2)-O(6) | 108.6(7) |
| $M(5)$ -O(24)w | 3.39(5) | | O(19)-Si(2)-O(9) | 110.0(9) |
| < $M(5)$ - ϕ > | 3.08 | | O(6)-Si(2)-O(9) | 110.8(9) |
| | | | <O-Si(2)-O> | 109.5 |
| $M(6)$ -O(15)t | 2.91(3) | x2 | | |
| $M(6)$ -O(20)s | 3.10(3) | x2 | O(26)q-Si(9)-O(26) | 107(4) |
| $M(6)$ -H ₂ O(27)b | 3.10(4) | | O(26),q-Si(9)-O(4),l | 108(2) |
| $M(6)$ -O(16),s | 3.28(3) | x2 | O(26)q-Si(9)-O(4),l | 108(2) |
| $M(6)$ -O(24)u | 3.33(5) | | O(4)-Si(9)-O(4) | 117(2) |
| < $M(6)$ - ϕ > | 3.13 | | <O-Si(9)-O> | 109 |
| | | | O(22)k-Si(10)-O(26) | 111(2) |
| | | | O(23)-Si(10)-O(11) | 101(2) |
| | | | O(22)k-Si(10)-O(23) | 104(2) |
| | | | O(11)-Si(10)-O(26) | 111(2) |
| | | | O(11)-Si(10)-O(22)k | 106(1) |
| | | | O(23)-Si(10)-O(26) | 122(2) |
| | | | <O-Si(10)-O> | 109 |

a = 1/2-x, 1-y, z, b = -x, 1/2-y, z, c = x+1/2, y-1/2, z, d = 1-x, 1/2-y, z, e = x+1, y, z, f = 1/2-x, y, z, g = -x, y-1/2, z, h = x, 1/2-y, z, i = -x, y+1/2, z, j = -x, y, -z, k = 1/2-x, 1/2-y, 1-z, l = x, 1/2-y, 1-z, m = x+1/2, 1/2-y, z, n = x, 1-y, z, o = x+1, -y, z, p = x-1/2, y, -z, q = -x, y, 1-z, r = 1-x, y-1/2, z, s = 1/2-x, -y, z, t = x, -y, z, u = -x, -y, -z, v = 1-x, y, 1-z, w = x+1/2, y+1/2, z

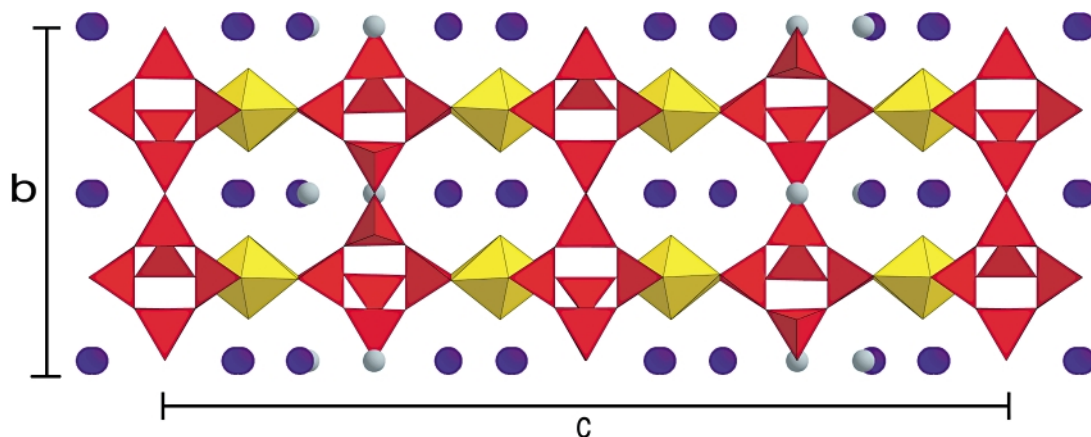


FIG. 1. Polyhedral representation of the structure of weeksite projected along [100]. The silicate tetrahedra are shown in red, the uranyl polyhedra are shown in yellow, purple spheres represent M sites (M : K, Ca and Ba), and bluish gray spheres represent the two symmetrically distinct H_2O groups.

site is displaced from the $4b$ position, with a Si(9)–Si(9) separation of 1.63(5) Å. The Si(8) and Si(10) sites are displaced from $8n$ positions, with Si(8)–Si(8) and Si(10)–Si(10) separations of 1.33(3) and 1.40(3) Å, respectively. Only one Si site of each pair may be occupied locally. The bond-valence sums incident at the Si positions, calculated using the parameters given by Brese & O’Keeffe (1991), range from 3.71 to 4.52 vu .

Low-valence cation sites

The structure contains six symmetrically distinct low-valence cation sites [labeled $M(1)$ to $M(6)$] in interstices within the uranyl silicate framework (Fig. 1). The $M(1)$ to $M(6)$ sites are each partially occupied.

The coordination polyhedra for the M sites are given in Table 4. The sites are coordinated by six to eight ligands, with mean bond-lengths in the range of 3.03 to 3.14 Å. The cation assignments for the M sites are discussed below.

Structural connectivity

The layer of uranyl and silicate polyhedra in the structure of weeksite is shown projected along [010] in Figure 2. The uranyl pentagonal bipyramids link by sharing edges to form chains one polyhedron wide that are parallel to [100]. Each uranyl polyhedron shares an edge with a silicate tetrahedron, with silicate tetrahedra staggered along the chain length. The resulting chain, with a U:Si ratio of 1:1, is common in uranyl silicates. It occurs in sheets based upon the uranophane anion-topology in α -uranophane, β -uranophane, sklodowskite $Mg[(UO_2)_2(SiO_3OH)_2](H_2O)_6$, cuprosklodowskite $Cu[(UO_2)_2(SiO_3OH)_2](H_2O)_6$, kasolite $Pb[(UO_2)(SiO_4)]$

H_2O , and boltwoodite (Burns *et al.* 1996), as well as in the more silica-rich sheet in the structure of haiweeite (Burns 2001). In the structure of weeksite, the uranyl silicate chains are linked together by the sharing of vertices of silicate and uranyl polyhedra with additional silicate tetrahedra, resulting in complex sheets that are similar to those found in haiweeite. In weeksite, however, the non-sheet vertices of the silicate tetrahedra bridge between adjacent sheets, resulting in an open uranyl silicate framework (Fig. 1).

Consider the bands of silicate tetrahedra that occur in the structure at $c = 0, \frac{1}{4}, \frac{1}{2}$ and $\frac{3}{4}$, between the chains of edge-sharing uranyl pentagonal bipyramids (Fig. 3). The bands at $c = \frac{1}{4}$ and $c = \frac{3}{4}$ may be described as crankshaft-like chains that contain four-membered rings of tetrahedra (at $a = 0$ and $a = \frac{1}{2}$) linked by vertex-sharing with additional tetrahedra on two sides (Fig. 3c). The bands at $c = 0$ and $c = \frac{1}{2}$ each involve displacement of two Si sites off special positions (Fig. 3b). These bands are also composed of crankshaft-like chains, but the two orientations shown in Figures 3c and 3d are superimposed, resulting in the split Si sites. The linkage of the crankshaft-like chains of silicate tetrahedra in the third dimension results in layers of six-membered rings parallel to (001) (Fig. 4).

The large, low-valence cations, K, Ca and Ba [labeled $M(1)$ to $M(6)$], and the two symmetrically distinct H_2O groups occupy channels in the framework (Fig. 1). $H_2O(28)$ is in the same plane as the six-member rings of silicate tetrahedra that are parallel to (001), and is connected to the structure only through hydrogen bonding (Fig. 4). $H_2O(27)$ is bonded to two cations, $M(1)$ and $M(6)$, at a distance of 2.78(4) Å and 3.10(4) Å, respectively.

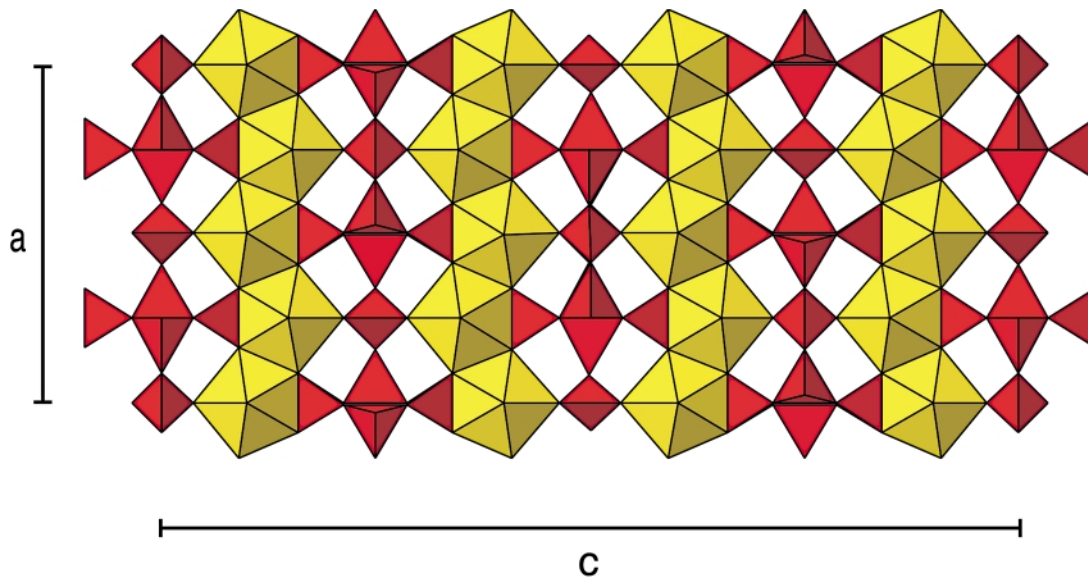


FIG. 2. Polyhedral representation of the uranyl silicate layer that occurs in weeksite, projected along [010]. Legend as in Figure 1.

TABLE 5. COMPOSITION OF WEEKSITE, AS DETERMINED BY ELECTRON-MICROPROBE ANALYSIS

| | | | |
|------------------------|-------------|------------------|--------------|
| Na ₂ O wt.% | 0.07 (0.04) | BaO | 3.72 (0.07) |
| K ₂ O | 4.85 (0.12) | UO ₃ | 58.36 (0.98) |
| CaO | 0.67 (0.21) | SiO ₂ | 29.93 (0.32) |
| SrO | 0.02 (0.01) | H ₂ O | 2.36 (0.92) |
| | | total | 99.98 |

Average result of eleven analyses from two different crystals of weeksite; the proportion of H₂O is assumed in order to give an analytical total of 100%. Estimated standard deviations (1σ) are shown in parentheses and represent the variability of the eleven datasets.

TABLE 6. PROPOSED CATION ASSIGNMENTS FOR THE M SITES IN WEEKSITE

| | Observed electron density | sof K | sof Ca | sof Ba | sof H ₂ O | Calculated electron density |
|-------------------|---------------------------|----------|-----------|-----------|-------------------------|-----------------------------|
| M(1) | 19.14 | 0.02 | 0.12 | 0.25 | 0.23 | 19.08 |
| M(2) | 20.03 | 0.02 | 0.12 | 0.25 | 0.33 | 20.08 |
| M(3) | 11.85 | 0.62 | | | | |
| M(4) | 10.67 | 0.56 | | | | |
| M(5) | 11.86 | 0.62 | | | | |
| M(6) | 12.13 | 0.64 | | | | |
| ½Σ _{sof} | | 1.24 | 0.12 | 0.25 | 0.28 | |

sof: site occupancy factor

Formula of the weeksite crystal studied

The average result of eleven electron-microprobe analyses of two crystals of weeksite is given in Table 5. The empirical formula is (K_{1.05}Ba_{0.25}Ca_{0.12}Na_{0.02})[(UO₂)_{2.08}(Si_{5.07}O_{12.38})](H₂O)_{1.46}, with H₂O assumed in order to give an analytical total of 100%. The EMPA data indicate that there is at most 0.03(11) wt.% Na and 0.00(14) wt.% Sr in the sample of weeksite studied; therefore, these elements were not considered when the chemical formula was recalculated. The site occupancies were refined for each M site using the atomic scattering factor for K. The total number of electrons associated with each M site was then calculated by multiplying the refined occupancy factor by 19, with the results presented in Table 6. The total number of electrons obtained for the M(1) and M(2) sites exceeds 19,

indicating that the Ba found in the EMPA is probably at these sites. We assumed that the Ca found in the EMPA is at the M(1) and M(2) sites, with Ba and Ca evenly distributed between the two sites. The remainder of the electron density at the M(1) and M(2) sites is assumed to be due to H₂O and small quantities of K. The remaining K obtained from the EMPA was assigned to the M(3) to M(6) sites in amounts appropriate for the observed number of electrons at each site (Table 6). This approach allowed us to account for the electron density observed at the M(1) to M(6) sites in a way that is consistent with the EMPA results, and that provides an electroneutral formula. The chemical formula of weeksite derived by combining the X-ray-diffraction data and the EMPA results is: K_{1.26}Ba_{0.25}Ca_{0.12}[(UO₂)₂(Si₅O₁₃)]H₂O.

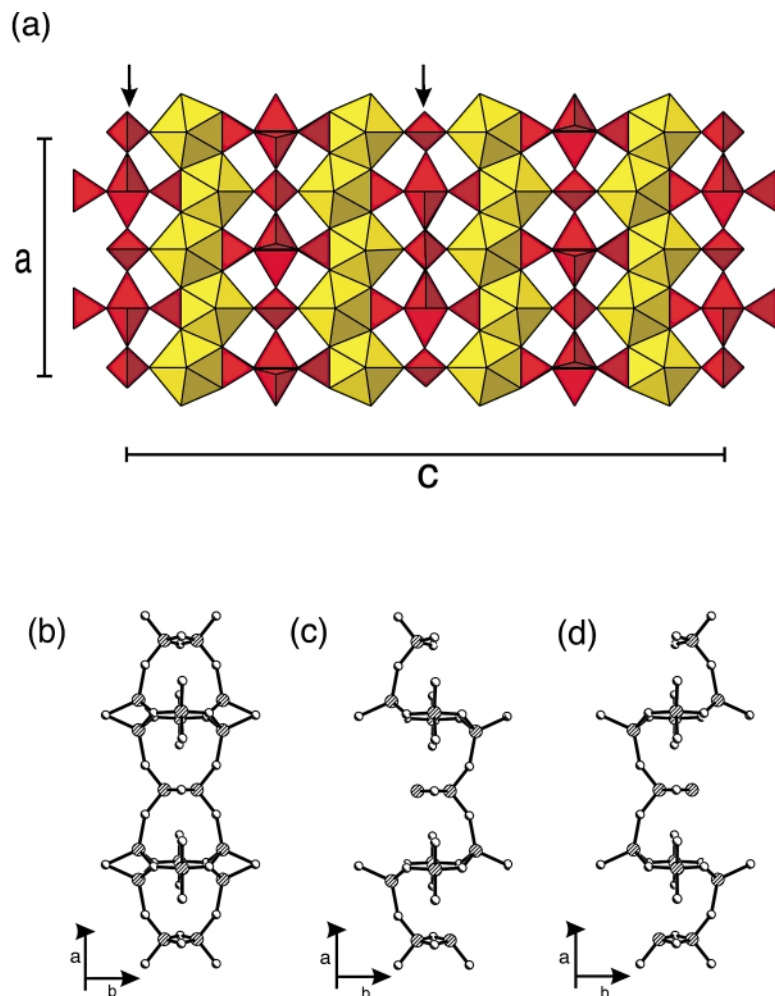


FIG. 3. Polyhedral representation of the uranyl silicate layer in weeksite (a). Chains of silicate tetrahedra that show split sites are indicated by arrows along [100] in (a). The chain shown in (b) contains split Si sites that arise from the occurrence of the orientations shown in (c) and (d). Legend for polyhedra as in Figure 1. Si cations are shown shaded with parallel lines, and O atoms are shown shaded in the lower-left corners.

RELATIONSHIP TO HAIWEEITE

The structure of haiweeite, which also has a U:Si ratio of 2:5, has structural features in common with weeksite (Burns 2001). It contains the same uranyl silicate layer as weeksite, although in haiweeite, the layers do not share vertices to form a framework as in weeksite. Rather, the layers in haiweeite are sheets that are connected through bonds to Ca cations and H₂O groups in the interlayer.

POTENTIAL INCORPORATION OF RADIONUCLIDES IN WEEKSITE

Incorporation of radionuclides in the structures of uranyl compounds that form during the alteration of nuclear waste in a geological repository may retard their release (Burns *et al.* 1997b, Burns 1999, Chen *et al.* 1999, 2000, Burns *et al.* 2000). Weeksite may form by the alteration of actinide-bearing borosilicate waste glass (Burns *et al.* 2000, Buck & Fortner 1997). As such,

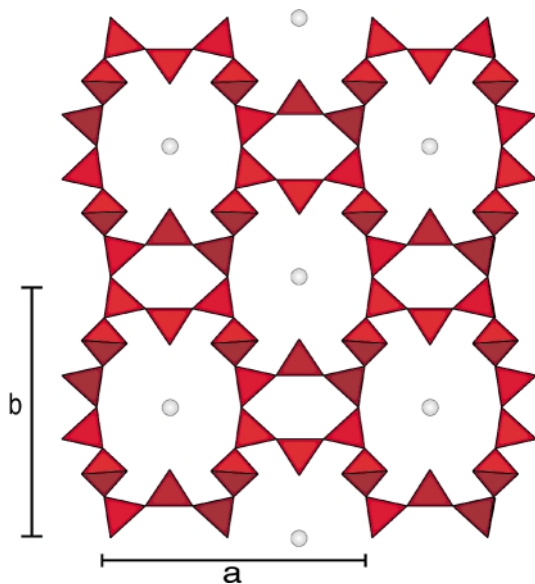


FIG. 4. Polyhedral representation of the six-membered rings of silicate tetrahedra that occur in weeksite, with the location of $\text{H}_2\text{O}(28)$ (gray spheres) in the plane of the rings. Legend as in Figure 1.

incorporation of transuranic elements into weeksite may have a significant impact on their release rates from the waste form.

First, consider the incorporation of Np^{5+} . The Np^{5+} cation invariably occurs in crystal structures as part of a nearly linear $(\text{NpO}_2)^+$ ion (Burns *et al.* 1997b). The neptunyl ion (*Np*) occurs in structures coordinated by four, five or six anions arranged at the equatorial corners of square, pentagonal and hexagonal bipyramids, analogous to the uranyl ion. However, the $\text{Np}-\phi$ bond lengths [$\phi = \text{O}^{2-}, \text{OH}^-, \text{H}_2\text{O}$] are slightly longer than those of $\text{U}-\phi$ in uranyl polyhedra [in $\text{Np}\phi_5$, $\langle \text{Np}-\text{O}_{\text{Np}} \rangle = 1.85(6) \text{ \AA}$ and $\langle \text{Np}-\phi_{\text{eq}} \rangle = 2.45(6) \text{ \AA}$] (Burns *et al.* 1997b). Given the geometric similarities of their coordination polyhedra, substitution of Np^{5+} for U^{6+} may be expected, assuming that a charge-balance mechanism is possible. Weeksite exhibits considerable chemical variability by substitution at the *M* sites (Outerbridge *et al.* 1960, Baturin & Sidorenko 1985), potentially providing a charge-balance mechanism. Using second difference electron-energy-loss spectroscopy (EELS), Buck & Fortner (1997) reported the incorporation of ~325(50) ppm Np into weeksite, which was identified by transmission electron microscopy (TEM) as an alteration phase on a corroded borosilicate glass (SRL 131) doped with actinides (0.01 wt.% Np) after ~1500 days of reaction.

The valence of Pu is variable, and there is uncertainty as to which valence state will dominate under the conditions of the proposed repository at Yucca Mountain. Polyhedron geometries for Pu^{4+} , Pu^{5+} , and Pu^{6+} in known structures were summarized by Burns *et al.* (1997b). The Pu^{4+} cation typically occurs in an approximately symmetric octahedral coordination, and as such is unlikely to substitute for U^{6+} in weeksite. In the case of both Pu^{5+} and Pu^{6+} , an approximately linear PuO_2 ion is present. In both cases, only hexagonal bipyramidal polyhedra have been observed, but the number of known structures is small. The substitution $\text{Pu}^{6+} \leftrightarrow \text{U}^{6+}$ should readily occur in weeksite, with the substitution $\text{Pu}^{5+} \leftrightarrow \text{U}^{6+}$ also possible, but requiring a charge-balance mechanism similar to the case of Np^{5+} .

The incorporation of Am^{3+} is most likely to occur in the low-valence interstitial cation sites in the weeksite structure, as it is incompatible with either the U^{6+} or Si^{4+} sites. Coordination polyhedra about Am^{3+} typically involve six to eight ligands at 2.35–2.55 Å (Burns *et al.* 1997b). Substitution of small quantities of Am^{3+} into any of the *M* sites in weeksite may occur, assuming that a charge-balancing mechanism also occurs.

ACKNOWLEDGEMENTS

The crystals of weeksite used in this study were provided by Dr. Mark Feinglos. We thank Bob Gault at the Canadian Museum of Nature, who provided results of preliminary electron-microprobe analyses, and Ian Steele at the University of Chicago for the microprobe data reported in this manuscript. We thank Paulus Moore and David Wronkiewicz for their comments and helpful suggestions on the manuscript, and Bob Martin for providing beneficial annotations. This research was funded by the Environmental Management Sciences Program of the United States Department of Energy (DE-FGO7-97ER14820).

REFERENCES

- BATURIN, S.V. & SIDORENKO, G.A. (1985): Crystal structure of weeksite $(\text{K}_{.62}\text{Na}_{.38})_2(\text{UO}_2)_2[\text{Si}_5\text{O}_{13}] \cdot 3\text{H}_2\text{O}$. *Sov. Phys. Dokl.* **30**, 435-437.
- BRESE, N.E. & O'KEEFFE, M. (1991): Bond-valence parameters for solids. *Acta Crystallogr.* **B47**, 192-197.
- BUCK, E.C. & FORTNER, J.A. (1997): Detecting low levels of transuranics with electron energy loss spectroscopy. *Ultramicroscopy* **67**, 69-75.
- BURNS, P.C. (1998): CCD area detectors of X-rays applied to the analysis of mineral structures. *Can. Mineral.* **36**, 847-853.
- _____ (1999): Cs boltwoodite obtained by ion exchange from single crystals: implications for radionuclide release in a nuclear repository. *J. Nucl. Mater.* **265**, 218-223.

- _____ (2001): A new uranyl silicate sheet in the structure of haiweeite and comparison to other uranyl silicates. *Can. Mineral.* **39** (in press).
- _____, EWING, R.C. & HAWTHORNE, F.C. (1997a): The crystal chemistry of hexavalent uranium: polyhedron geometries, bond-valence parameters, and polymerization of polyhedra. *Can. Mineral.* **35**, 1551-1570.
- _____, _____ & MILLER, M.L. (1997b): Incorporation of actinide elements into the structures of U^{6+} phases formed during the oxidation of spent nuclear fuel. *J. Nucl. Mater.* **245**, 1-9.
- _____, MILLER, M.L. & EWING, R.C. (1996): U^{6+} minerals and inorganic phases: a comparison and hierarchy of crystal structures. *Can. Mineral.* **34**, 845-880.
- _____, OLSON, R.A., FINCH, R.J. & HANCHAR, J.M. (2000): $KNa_3(UO_2)_2(Si_4O_{10})_2(H_2O)_4$, a new compound formed during vapor hydration of an actinide-bearing borosilicate waste glass. *J. Nucl. Mater.* **278**, 290-300.
- CHEN, F., BURNS, P.C. & EWING, R.C. (1999): ^{79}Se : geochemical and crystallo-chemical retardation mechanisms. *J. Nucl. Mater.* **275**, 81-94.
- _____, _____ & _____ (2000): Near-field behaviour of ^{99}Te during the oxidative alteration of spent nuclear fuel. *J. Nucl. Mater.* **278**, 225-232.
- FINCH, R.J., BUCK, E.C., FINN, P.A. & BATES, J.K. (1999): Oxidative corrosion of spent UO_2 fuel in vapor and dripping groundwater at 90°C. *Mat. Res. Soc., Symp. Proc.* **556**, 431-438.
- _____, & EWING R.C. (1992): The corrosion of uraninite under oxidizing conditions. *J. Nucl. Mater.* **190**, 133-156.
- _____, & MURAKAMI, T. (1999): Systematics and paragenesis of uranium minerals. In *Uranium: Mineralogy, Geochemistry and the Environment* (P.C. Burns & R. Finch, eds.). *Rev. Mineral.* **38**, 91-179.
- FRONDEL, C. (1958): Systematic mineralogy of uranium and thorium. *U.S. Geol. Surv., Bull.* **1064**.
- IBERS, J.A. & HAMILTON, W.C., eds. (1974): *International Tables for X-Ray Crystallography IV*. The Kynoch Press, Birmingham, U.K.
- MANDARINO, J.A. (1999): *Fleischer's Glossary of Mineral Species*. Mineralogical Record, Tucson, Arizona.
- OUTERBRIDGE, W.F., STAATZ, M.H., MEYROWITZ, R. & POMMER, A.M. (1960): Weeksite, a new uranium silicate from the Thomas Range, Juab County, Utah. *Am. Mineral.* **45**, 39-52.
- PEARCY, E.C., PRIKRYL, J.D., MURPHY, W.M. & LESLIE, B.W. (1994): Alteration of uraninite from the Nopal I deposit, Peña Blanca District, Chihuahua, Mexico, compared to degradation of spent nuclear fuel in the proposed U.S. high-level nuclear waste repository at Yucca Mountain, Nevada. *Appl. Geochem.* **9**, 713-732.
- POUCHOU, J.-L. & PICOIR, F. (1984): A new model for quantitative X-ray microanalysis. 1. Application to the analysis of homogeneous samples. *Rech Aérosp.* **3**, 14-38.
- STOHL, F.V. & SMITH, D.K. (1981): The crystal chemistry of the uranyl silicate minerals. *Am. Mineral.* **66**, 610-625.
- WILSON, C.N. (1990): Results from NNWSI Series 3 spent fuel dissolution tests. *Pacific Northwest National Laboratory, Richland, Washington, Tech. Rep. PNL-7170*.
- WRONKIEWICZ, D.J., BATES, J.K., WOLF, S.F. & BUCK, E.C. (1996): Ten-year results from unsaturated drip tests with UO_2 at 90°C: implications for the corrosion of spent nuclear fuel. *J. Nucl. Mater.* **238**, 78-95.

Received August 19, 2000, revised manuscript accepted December 30, 2000.